Journal of Chromatography B, 879 (2011) 2095–2106

Contents lists available at ScienceDirect

Journal of Chromatography B

journal homepage: www.elsevier.com/locate/chromb

Glycerophosphocholine molecular species profiling in the biological tissue using UPLC/MS/MS

Chuan-Ho Tang[a,b,c], Po-Nien Tsao[d], Chia-Yang Chen[a], Ming-Shi Shiao[e], Wei-Hsien Wang[b,f], Ching-Yu Lin[a,*]

[a] Institute of Environmental Health, College of Public Health, National Taiwan University, 17 Hsuchou Rd., Taipei City 100, Taiwan
[b] National Museum of Marine Biology and Aquarium, 2 Houwan Rd., Checheng, Pingtung 944, Taiwan
[c] Institute of Marine Biodiversity and Evolutionary Biology, National Dong Hwa University, 2 Houwan Rd., Checheng, Pingtung 944, Taiwan
[d] Department of Pediatrics, National Taiwan University Hospital, 7 Chungshan South Rd., Taipei City 100, Taiwan
[e] Department of Biomedical Sciences, Chang Gung University, 259 Wenhwa 1st Rd., Kweisan, Taoyuan 333, Taiwan
[f] Asia-Pacific Ocean Research Center, National Sun Yat-Sen University, 70 Lien-hai Rd., Kaohsiung 804, Taiwan

ARTICLE INFO

Article history:
Received 23 March 2011
Accepted 31 May 2011
Available online 12 June 2011

Keywords:
Glycerophosphocholine profiling
Electrospray ionization
Triple quadrupole mass spectrometer
UPLC

ABSTRACT

A strategy consisting of a two-phase analytical procedure was used to obtain detailed molecular species composition for glycerophosphocholines (GPCs) profiling in biological tissue using ultra performance liquid chromatography coupled with a triple quadrupole mass spectrometer operating under electrospray mode. In phase one of the analytical procedure, the precursor ion scan was first conducted to obtain the preliminary lipid profile that revealed the composition of the molecular species possessing phosphocholine structure in the biological tissue. In phase two of the analytical procedure, each product ion spectrum obtained for the GPC components in the profile was sequentially acquired for the determination of the molecular structure. A simple guide with high differentiability was proposed for the diacyl-, alkyl-acyl- and alk-1-enyl-acyl-GPC, and related lyso-GPCs molecular structure decision. Total 93 GPCs molecular species were identified in the fetal mouse lung with the relative amounts from 14.39% to less than 0.01% (normalizing by the total GPCs signal). The optimized chromatographic conditions were also proposed in the analytical procedure based on the compromise between the separation efficiency and electrospray signal response. The plate number of the probing GPCs was obviously improved to above 30,000 and the detection limits of the probing GPCs were between 0.002 and 0.016 ng/μL. The practical usability of the analytical procedure has been validated using a study of chemically induced early lung maturation. The metabolic difference between chemically treated and untreated fetal mouse lung was clearly distinguished by the composition of GPCs with several characteristics of molecular structure. The overall results showed that this two-phase analytical procedure was reliable for comprehensive GPC profiling.

1. Introduction

The glycerophospholipids, such as glycerophosphocholines (GPCs), glycerophosphoethanolamines, glycerophosphoserines and others, are the major structural lipids in eukaryotic membranes and GPCs generally account for more than 50% [1]. GPCs are composed of a glycerol backbone with one phosphocholine head group at the *sn*-3 position and fatty acid substituent at the *sn*-1 and/or *sn*-2 position; the fatty acid substituent can be esterified (acyl-) at both positions and can also either be a long-chain alkyl ether (O-alkyl-) or vinyl ether (O-alk-1′-enyl-) substituent at the *sn*-1 position. The diradyl-GPCs (PCs) can be divided into three subclasses, owing to the difference of linkage at *sn*-1 position, phosphatidylcholine (1,2-diacyl-GPC), plasmanylcholine (1-O-alkyl-2-acyl-GPC), and plasmenylcholine (1-O-alk-1′-enyl-2-acyl-GPC). Another type of GPCs is lyso-GPCs (LPCs), which possessed one glycerol hydroxyl substituent at either the *sn*-1 or *sn*-2 position instead of the esterified linking fatty acid substituent. In addition to the different linkages of fatty acids, the diversity of GPCs molecular species can also be attributed to the number of carbon and double bonds in the fatty acid substituent and the substituents' location on the glycerol backbone.

Abbreviations: ACN, acetonitrile; GPC, glycerophosphocholine; HPLC/MS/MS, high-performance liquid chromatography with tandem mass spectrometry; LOD, limit of detection; LPC, lyso-glycerophosphocholine; MeOH, methanol; PCA, principal components analysis; UPLC, ultra performance liquid chromatography; VEGF, vascular endothelial growth factor.

* Corresponding author. Tel.: +886 2 33668099.
E-mail address: chingyulin@ntu.edu.tw (C.-Y. Lin).

1570-0232/$ – see front matter © 2011 Elsevier B.V. All rights reserved.
doi:10.1016/j.jchromb.2011.05.044

The physical properties of GPCs are dependent on distinctions of their chemical structures, which make them functionally diverse in biological systems [2,3]. The cellular lipids complement provides an appropriate hydrophobic environment for many membrane proteins to function and interact through membrane dynamics; these lipids take advantage of basic principles of physical chemistry and regulate the physiologic function and adaptation for the living cells [4]. Certain cellular membrane properties are distinguished by a specific composition of molecular species for PCs [5,6] in which the physiological function of PCs can be characterized. Besides, the condition, state, and dysfunction of cells can also be detected through variations in the molecular characteristics of the PCs. LPCs are a representative class of biochemical intermediates that are involved in PC metabolism and the remodeling of the biosynthetic pathway. LPCs could be produced via the enzymatic hydrolysis of PCs, such as by numerous phospholipase A_1 or A_2 enzymes [7] and they can also be readily reacylated to produce PCs by either CoA dependent or CoA independent pathways [8,9]. Because LPCs do not form regular membrane bilayer structures, cellular functions would be altered when the membrane compositions of LPCs change even by small quantities [10]. The unique biophysicochemical properties of LPCs have revealed considerable interest in the cellular action process in which variations of LPCs have been regarded as important events, such as the fusion of membranes in the process of endocytosis or exocytosis [11,12]. In addition, the LPCs also act as the second messengers that participate in the cellular signaling functions [13]. The specific lipid composition presented in the cell may impinge on the variation of life processes. Consequentially, a composition analysis that detailed the lipid molecular species has formed an active research field in cellular biochemistry that is important for the understanding of various cellular processes. Researchers have demonstrated the importance of GPCs in the study of clinical medicine, pharmacology, and basic research in which the changes of GPCs have been correlated with the cell membrane structure and functions [14–16].

Several analytical strategies are available for GPC analysis. Conventional strategies for the composition measurement of glycerophospholipid molecular species require a series of chemical treatment procedures prior to analysis [17]. Briefly, the separation step of lipid class and its molecular species should be done first and followed by the saponification and esterification steps to obtain the fatty acid methyl esters for the gas chromatographic analysis. The lipid molecular species can be described by the level of fatty acid substituents that are attached on the glycerol backbone; however, the information of the linkage position is absent. These pre-treatment procedures are quite taxing and often suffer from the loss of certain lipid molecular species [18].

The technique of high-performance liquid chromatography (HPLC) coupled with tandem mass spectrometry (HPLC/MS/MS) provides an excellent solution to directly determine the composition of lipid molecular species in the total lipid extracts [19–21]. An HPLC/MS/MS equipped with an electrospray ionization source can be used to deal with the complex mixtures of lipid extracts, which can provide high selectivity and sensitivity of signal response. Based on the combination of chromatographic separation and unique collision-induced fragmentation pathways, the comprehensive glycerophospholipid profiling can be done rapidly. Reversed-phase HPLC has been a primary choice for the separation of molecular species via the lipophilic partition mode. In fact, the reversed-stationary phase is the primary method used for separations on HPLC apparatuses today. The intact GPCs have also been successfully analyzed using this separation technique. However, long separations times (greater than one half hour) were typically required and imperfect separation resolution were obtained due to the strong retention and/or second retention by the alkylsilica stationary-phase, which caused peak broadening and tailing in the separation of GPCs and glycerophosphoethanolamines, even after the optimization of separation conditions [22]. Recent advances in the chromatographic systems have led to the achievement of high peak resolution within several minutes of analysis time. Superior separations and increased sensitivity are obtained due to this elevated chromatographic efficiency with a short time demand [23]. This “Ultra Performance” liquid chromatography (UPLC) builds on the same principles of HPLC, but a sub-2 μm diameter particle size is employed as the stationary phase and it is operated at high pressures that account for more than 10,000 psi. Owing to high complexity presented in the component of total lipid extracts, UPLC has recently been considered an infuser for the electrospray ionization mass spectrometry to provide an excellent profile of lipid molecular species. Although the HPLC/MS/MS has successfully been used to analyze GPCs [24], long analysis time is needed and errors of the quantification and loss of the minor molecular species is probably due to the restricted chromatographic efficiency.

In this study, the usefulness of the coupling of UPLC/MS/MS with an electrospray interface in reversed-phase separation mode was demonstrated for GPCs profiling of biological tissue. A strategy for the two-phase analytical procedure was adopted to survey the composition of the GPC molecular species by way of both the precursor ion scan (phase one) and the sequential acquirement of the product ion spectra (phase two). A problem existed in the process of the UPLC separation before conditions were optimized that caused peak broadening and tailing of the phosphocholines (GPCs and sphingomyelin), which occurred when using a octadecylsilica column for the chromatography. This was consistent with previous HPLC separation studies [22]. Hence, the optimization of chromatographic conditions must be performed prior to performing the sample analysis. The choice of the mobile phase composition depended on the chromatographic efficiency and also the signal response of the electrospray ionization, which is generally composed of the simplest combination of solvents possible. In addition, a simple guide with high differentiability for determining the molecular structure of GPCs was proposed based on the acquisition of the product ion spectra that were derived from collision-induced fragmentations with a specific energy. The performance analysis of the procedure was described and the practical usability was validated through a study of chemically induced early lung maturation in the premature mouse model. The analytical procedure proposed here should be useful for lipidomic research.

2. Materials and methods

2.1. Chemicals

All lipid standards were purchased from Avanti Polar Lipids (Alabaster, AL, USA). LC/MS grade methanol (MeOH), acetonitrile (ACN), and analyzed ACS reagents of chloroform were obtained from J.T. Baker (Phillipsburg, NJ, USA). Ammonium acetate (LC/MS grade) was acquired from Sigma–Aldrich (St. Louis, MO, USA), sodium chloride (ACS grade) was obtained from Merck (Darmstadt, Germany) and purified distilled water was obtained from a Milli-Q system of Millipore (Milford, MA, USA).

The designations and abbreviations of GPCs are according to the recommendation by LIPID MAPS (i.e., 1,2-dihexadecanoyl-, 1-hexadecyl-2-hexadecanoyl-, and 1-(1Z-hexadecenyl)-2-hexadecanoyl-*sn*-glycero-3-phosphocholine are respectively abbreviated as PC(16:0/16:0), PC(O-16:0/16:0), and PC(P-16:0/16:0)). These GPCs possessed the fatty acid chain at both the *sn*-1 and *sn*-2 positions of the glycerol backbone that are collectively named PCs in this study. The notation *x*:*y* for a fatty acid chain indicated the number of carbons (*x*) and double bonds (*y*); additionally, symbols marked with ‘O’ or ‘P’ indicated

the fatty acid chain link with the glycerol backbone via alkyl ether or vinyl ether in general at the *sn*-1 position, without any marks indicating an ester linkage. The glycerol backbone of GPCs possessing a hydroxyl substituent at either the *sn*-1 or *sn*-2 position was named lyso-GPCs (LPCs), i.e., 1-hexadecanoyl-2-hydroxyl-*sn*-glycero-3-phosphocholines could be abbreviated as PC(16:0/0:0).

2.2. UPLC/MS/MS experiment for GPCs profiling

A strategy consisting of a two-phase analytical procedure was used to obtain a detailed molecular species composition for glycerophosphocholines (GPCs) profiling in the biological tissue. The GPCs composition could be profiled and identified through unique fragmentation pattern in their product ion spectra. The GPCs have a common feature on the head group with the formation of a obvious ion signal at *m*/*z* 184, corresponding to the phosphorylcholine ion in their product ion spectra of the protoned molecular ion ($[M+H]^+$). In phase one of the analytical procedure, hence, the preliminary profiling of GPCs can be obtained via a precursor ion scan of *m*/*z* 184 in the positive ion mode. Although the protoned sphingomyelin (SM, ceramide phosphocholines, such as N-(heptadecanoyl)-sphing-4-enine-1-phosphocholine, could be abbreviated as SM(d18:1/17:0)) also produced a phosphorylcholine ion signal in its product ion spectra, its *m*/*z* in odd units were different from GPCs. Subsequently, in phase two of the analytical procedure, another UPLC/MS/MS experiment based on the preliminary GPCs profile was conducted to acquire the product ion spectra for the GPCs molecular structure determination. The product ion scan in a specific *m*/*z* of molecular species was conducted according to its chromatographic retention time. Thus, the molecular structure of GPCs could be determined by illustrating the product ion spectra of $[M+H]^+$, $[M+Na]^+$, and $[M-Me]^-$ ions.

A Waters Acquity UPLC system, coupled with a Waters Quattro Premier XE triple quadrupole mass spectrometer (Waters, Milford, MA, USA), was used to perform the GPCs profiling. Reversed-phase chromatography was operated on a Waters BEH C_{18} 1.7 μm, 2.1 mm × 100 mm, analytic column using the binary solvent systems A: 10 mM NH_4Ac in water and B: ACN/MeOH (65/35) containing 1% 1.0 M NH_4Ac. The lipid extracts of the tissue (10 μL) were analyzed with the column eluting at a constant flow rate of 0.7 mL/min and column temperature at 70 °C. The gradient elution, solvent B was programmed to increase from 35% to 70% in 0.1 min, then to 100% in 1.4 min, and hold at 100% for 4.5 min.

The optimized operation conditions were respectively set in the MS experiments to obtain better signal sensitivity for the analysis of the preliminary profiling and product ion spectra. The desolvation was operated with a N_2 gas flow at 700 L/h under 450 °C and the ion source temperature was set at 120 °C with a 50 L/h cone gas flow set for all MS experiments. For the preliminary GPCs profiling, the capillary and sampling cone voltages were set at 2.5 kV and 35 V, respectively with collision energy of 30 eV to conduct the precursor ion scan of *m*/*z* 184. These parameters were also used in the $[M+H]^+$ ions of the product ion scan for the LPCs molecular structure determination. The $[M+Na]^+$ ions were sampled by capillary and cone voltages of 2.5 kV and 45 V, respectively; a collision-induced fragmentation with collision energy of 28 eV was then performed to produce the product ion spectra for the determination of the class of PCs. The product ion spectra of the $[M-Me]^-$ ions were acquired using capillary and cone voltages of 3.0 kV and 50 V, respectively, with a collision energy of 30 eV in the negative ion mode for the assignment of the fatty acid substituent for the molecular structures of the PCs. As collision gas, Ar flow rate was set at 0.1 mL/min in the MS experiments.

The performance and validation of the analytical procedure was performed at each batch run. Every lipid extract of the tissue was spiked with equivalent external standards, namely SM(d18:1/17:0) and PC(17:0/0:0), prior to UPLC/MS/MS analysis to correct for possible variations in the signal response during the instrument measurement. The added external lipid standards were picked according to their masses and expected retention times. These lipid standards were used to normalize the signal of the GPCs to adjust the precision between each sample run. Calibration curves were determined using GPC standards to confirm the linear range of signal response and instrumental sensitivity. Quantitative recoveries of GPC extractions were performed in three replicate measurements of samples spiked with GPC standards to determine extraction efficiency and precision. Limits of detection were based on three times the standard deviation of seven replicate experiments with the standard solution.

2.3. Application of the UPLC/MS/MS method to lung samples

2.3.1. Animal treatment

Previous study shows vascular endothelial growth factor (VEGF) treatment improved fetal lung maturation in premature mice [25]. To follow that study, we injected VEGF agonist intra-amniotically at E17.5 for half number of fetus to improve fetal lung maturation and the other fetus were injected saline as control in one pregnant mouse. The pups were delivered prematurely by C-section at E18.5. After birth, the fetal lungs were homogenized and the contents of the GPCs were analyzed. The profiling of the GPCs for all samples of fetal mouse lung was conducted by three replicate measurements in the present study. The variation of analysis for GPC profiling was determined prior to the experiment by the three replicate measurements of another eight E18.5 fetal mice lungs delivered from the same pregnant mouse.

2.3.2. Lipid extraction from lung tissue

The lung sample pretreatment and lipid extraction method was previously published [26,27] and used with some modification. Briefly, frozen lung tissues were ground in a liquid N_2-cooled mortar and lyophilized overnight. The homogenous dry tissue powder (1.0 mg) was weighed and then extracted with chloroform/methanol (2/1) (0.6 mL) by shaking for 10 min. The mixture was then mixed thoroughly with 0.15 mL of 0.05 M NaCl solution. Following centrifugation (10,000 × *g*, 10 min, 4 °C), the entire lower layer was collected and then dried. The dried lipid extracts was redispersed with methanol and frozen at −80 °C until further analysis.

2.3.3. Data analysis on the lung samples

LC/MS data acquisition generally shows less stability and reproducibility. Therefore, equivalent SM(d18:1/17:0) and PC(17:0/0:0) was spiked in each lipid extract of the lung tissue prior to UPLC/MS/MS analysis for evaluation of the time shifts of peak elution and variations in signal sensitivity. The mass/retention time pairs derived from the profile of the GPCs were taken as variable for statistical analysis. The picked peak responses of PCs and LPCs were respectively scaling to SM(d18:1/17:0) and PC(17:0/0:0) lipid standard, in which the ratio of average response of lipid standard in each batch run to the single response of lipid standard in the sample was calculated as a scale factor and applied to each single variable in the sample. In the present study, the same weight of lung tissue for each sample was used to carry out the chemical analysis, no additional normalization was perform.

Principal component analysis (PCA) was conducted to determine whether the metabolic turbulences of the GPCs caused by the treatment can be distinguished using the SPSS 16.0 statistical software (SPSS Inc., Chicago, IL, USA). PCA, an unsupervised method, can identify the directions of maximum variances in a data set without relating to the classic labels. PCA reduce dimension from the multidimensional data set that converts correlated variables into a fewer

number of mutually linearly orthogonal variables called principal components. The first principal component describes the largest variation in the data set, following the second principal component describing the second largest variation and so on. This pattern recognition method summarized the original variables to fewer variables based on their weighted averages. The new variables were also called scores and the weighted profiles were called loadings. Each GPC profile was represented by single point in a scatter plot of the first two score vectors and the data set was displayed as the swarm of points. The position of each point in the score plot was used to relate to each other in which points that are cluster together have a similar GPC profile. Conversely, points far from each other indicate dissimilar properties. Potential outliers and the degree of similarity between the GPC profiles could be identified. Similar to the scores, the loading vectors describe the relation among the measured variables, which loading plot shows the information about GPC molecular species that contribute to the point separation in the score plot. The feature is shown that directions in the loading plot correspond to directions in the score plot for identifying which GPC molecular species were responsible for the separation in the data set.

3. Results and discussion

3.1. Optimization of chromatographic conditions

The chromatograms obtained using differential compositions of the mobile phase are presented in Fig. 1 to illustrate the improvement on the peak characteristic of phosphocholines with the association of a suitable ACN/MeOH mixture and NH_4Ac content. It was evident that using an optimized combination of the mobile phase led to a great increase of peak symmetry and resolution of the PCs and SM with a concurrent decrease in retention times (Fig. 1C). An insufficient amount of MeOH (Fig. 1A) or NH_4Ac content (Fig. 1B) in the mobile phase for chromatography caused the PCs and SM to strongly adsorbed on the stationary phase and gave peak broadening and tailing. The components of PCs and SM were too broad to be quantifiable in the absence of either MeOH or NH_4Ac in the mobile phase. The broadened peak of the LPCs was also observed using differential ACN/MeOH ratios as the mobile phase in the absence of NH_4Ac. However, the narrow peaks of the LPCs were obtained while few NH_4Ac were present in the mobile phases. The present study used an octadecylsilica column for the separation of the phosphocholines. In alkyl-chain bonded columns, the residual silanols on the stationary phase can interact with polar compounds in the chromatographic process through hydrogen bond and dipole–dipole interactions. This type of heterogeneous surface on the stationary phase often causes unsatisfactory chromatography, particularly for solutes that possess positive charge. The phosphocholines are internally neutral molecules and simultaneously possess a positive and negative charge. Hence, the peak tailing and broadening caused by phosphochlines in the chromatography can be partly contributed by the interactions with residual silanols. PCs and SM react very strongly with these silanols due to their greater degree of hydrophobicity, which leads to a greater diffusion coefficient for the bonded ligands and allow greater penetration of them to the silanols [28]. Therefore, the present study attempted to combine suitable organic solvent modifiers and salt additives in the mobile phase to improve the chromatographic separation of phosphocholines. The results indicated that an improvement in the chromatography was obtained by using sufficient amount of MeOH and NH_4Ac in the mobile phase in the correct ratio.

Fig. 2 shows a plot of the plate number, calculated using the half-height method, vs. the NH_4Ac content in the mobile phase, which revealed more efficient chromatography for LPCs when the

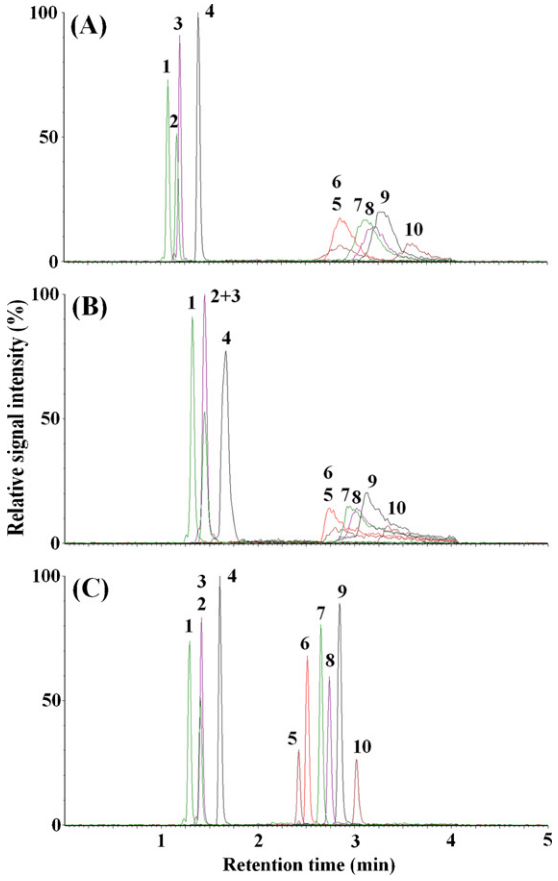

Fig. 1. Extracted ion chromatogram of the UPLC/MS separation of phosphocholines using a differential composition of the mobile phase with a flow rate of 0.7 mL/min at 70 °C. (A) ACN/MeOH (90/10) with 1.0% of 1.0 M NH_4Ac; (B) ACN/MeOH (65/35) with 1.0% of 2.0 mM NH_4Ac; (C) ACN/MeOH (65/35) with 1.0% of 1.0 M NH_4Ac. The analysis of the phosphocholines included the following: 1, PC(16:0/0:0); 2, PC(17:0/0:0); 3, PC(O-16:0/0:0); 4, PC(P-18:0/0:0); 5, SM(*d*18:1/17:0); 6, PC(16:0/16:0); 7, PC(O-16:0/16:0); 8, PC(17:0/17:0); 9, PC(P-18:0/18:1); 10, PC(18:0/18:0).

NH_4Ac content was above 0.2 mM. The plate number increased with of NH_4Ac content in the mobile phase for PCs and SM; this was more obvious compared to LPCs where the plate number increased 20–70 times for PCs and SM following the increase of NH_4Ac content from 0.02 to 10 mM. While NH_4Ac content was above 10 mM in the mobile phase, the maximum chromatographic efficiency for PCs and SM were reached. In addition to NH_4Ac content, the MeOH ratio

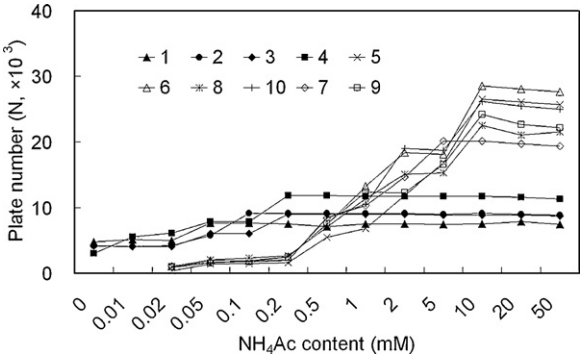

Fig. 2. The effect of NH_4Ac content on the ACN/MeOH (65/35) mobile phase for the chromatographic analysis of the phosphocholines with a flow rate of 0.7 mL/min at 70 °C. The analysis of the phosphocholines included the following: 1, PC(16:0/0:0); 2, PC(17:0/0:0); 3, PC(O-16:0/0:0); 4, PC(P-18:0/0:0); 5, SM(*d*18:1/17:0); 6, PC(16:0/16:0); 7, PC(O-16:0/16:0); 8, PC(17:0/17:0); 9, PC(P-18:0/18:1); 10, PC(18:0/18:0).

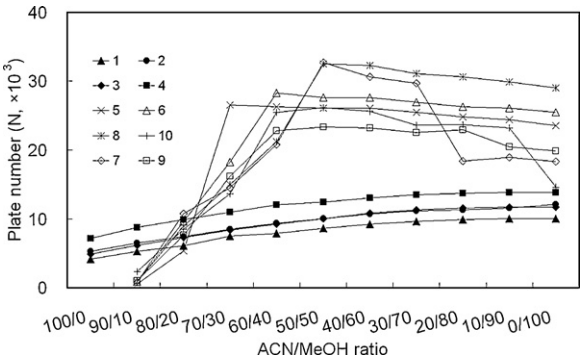

Fig. 3. The effect of the ACN/MeOH composition on the mobile phase (with 1.0% of 1.0 M NH_4Ac) for the chromatographic determination of phosphocholines with a flow rate of 0.7 mL/min at 70 °C. The analysis of the phosphocholines included the following: 1, PC(16:0/0:0); 2, PC(17:0/0:0); 3, PC(O-16:0/0:0); 4, PC(P-18:0/0:0); 5, SM(*d*18:1/17:0); 6, PC(16:0/16:0); 7, PC(O-16:0/16:0); 8, PC(17:0/17:0); 9, PC(P-18:0/18:1); 10, PC(18:0/18:0).

in the mobile phase was also a critical factor for chromatographic efficiency of the phosphocholines. As shown in Fig. 3, the change of the MeOH ratio in the mobile phase revealed obvious influence in the chromatographic efficiency for PCs and SM. The plate number increased 10–50 times with an increase in the MeOH ratio from 10% to 30–50%. However, the plate number notably decline while the MeOH ratio was raised above 70% and 90% in the mobile phase for PC(O-16:0/16:0) and PC(18:0/18:0), respectively. Clearly, a range of 40–70% was preferable MeOH ratio for the mobile phase for the separation of PCs and SM based on the chromatographic efficiency. For LPCs, the equal increase in plate number with increasing MeOH ratio was observed; plate number increased in retention time with relative constant peak width. The NH_4Ac could be effective in alleviating the interactions between the phosphocholines and residual silanols by way of ion suppression [22]; immediate results were visible in the chromatography for LPCs. Although clearly alleviated when enough NH_4Ac was presented in the mobile phase, the peak tailing of PCs and SM show contrast when Fig. 1A and B are compared. Compared to LPCs, enough MeOH needed to be presented in the mobile phase to get a good chromatography data for the PCs and SM; this is because bonded ligands modified by the sorption of MeOH had greater hydrogen bond donor acidities in contrast with those modified by ACN. Thus reduce hydrophobic interaction with PCs and SM also implies a diminution in the diffusion coefficient of PCs and SM on the bonded ligands [29]. This effect of MeOH on the chromatography was revealed with the shorter retention of the PCs and SM in Fig. 1B compared to Fig. 1A. Thus, broader peaks and more retention of LPCs were obtained using higher MeOH ratio in the mobile phase due to the increase in diffusion coefficient of LPCs on bonded ligands with more MeOH solvation. This should be attributed to the hydroxyl group that LPCs possess and a lesser degree of hydrophobicity. An alternative explanation could be that the PCs and SM were more solvated with MeOH compared to the LPCs interacting with ACN in which the diffusion coefficient in the mobile phase increased when the favorable solvent modifier was predominant. The change of the solute diffusion coefficient could be due to a combined effect in bonded ligand modifications and solute solvation by the solvent modifiers in the mobile phase. The effect of pH on the chromatographic efficiency for phosphocholines has also been tested via the addition of different amounts of acetic acid or ammonium hydroxide in the mobile phase that were composed of the ACN/MeOH (65/35) with 10 mM NH_4Ac. The variation of pH value, measured in the aquatic mobile phase in the range of 3.71–10.21 did not significantly affect on the chromatographic efficiency for the phosphocholines (the data not shown).

Tuning the flow rate and column temperature could be beneficial in increasing chromatographic efficiency and save time, both conditions had also been optimized in this study (the data not shown). The solute chromatographic band was broader at low flow rate, which is prone to a longer time for longitudinal diffusion of the solutes in the column. The solute band broadening was also evident at high flow rates due to time lags caused by the inadequate phase diffusion between the mobile and the stationary phases in the chromatographic process. The column temperature had a clear effect on the diffusion coefficients of the solute in which the response towards temperature change was solute-dependent. In generally, the solute diffusion in and out of the stationary phase could be accelerated at higher temperatures and a higher flow rate can be adopted to reduce the chromatographic time. Moreover, a higher temperature can reduce the viscosity of mobile phases, and then results in a lower back pressure; thus, a higher flow rate can be adopted without exceeding the tolerable pressure of the instrument. The decision of conditions for the chromatographic resistance of mass transfer and molecular species complexity of phosphocholines in biological tissues depended on desirable plate number for PCs and SM. Fig. 1C illustrates a good chromatogram obtained using 10 probes of phosphocholines within a 3.5 min elution time, where the optimal conditions had be used.

3.2. Effect of composition on the mobile phase for signal response

The composition of the mobile phase was known to have an obvious effect on the signal intensity of the LC/MS equipped with an electrospray ionization interface. Fig. 4 shows the effect of the mobile phase constituted with different ACN/MeOH ratios for the signal response of phosphocholines in peak height. Results for the $[M+H]^+$, $[M+Na]^+$ and $[M-Me]^-$ ion intensities of PCs and SM showed similar track changes with increased amounts of MeOH in the mobile phase. The highest response peaked was obtained with a mobile phase consisting of 70/30–60/40 ACN/MeOH. Further increasing the MeOH content caused an obvious signal drop, especially for $[M-Me]^-$ ions, followed by slight variations in the signal response between ratios of 40/60–0/100 ACN/MeOH. Increasing the MeOH ratio in the mobile phase was useful for the improvement of the peak shape for PCs and SM in which the signal sensitivity was simultaneously elevated. Compared with ACN, nevertheless, MeOH is more polar and its viscosity is higher, which was unfavorable in the process of electrospray ionization (i.e., in the solvent evaporation and formation of small droplets) [30]. Moreover, PCs and SM ions were solvated favorably with MeOH via the oxygen–hydrogen binding interactions, which prefer to be away from the droplet surface and reduced the efficiency in the production of the gaseous ion from the charged droplet [31]. Higher MeOH ratios induced a signal decrease for the $[M-Me]^-$ ion that may also be related to its higher dielectric constant. The LPCs' change in $[M+H]^+$ and $[M-Me]^-$ ion intensities showed a trend of moderate decline with an increase of MeOH ratio in the mobile phase. This decline was less for the LPCs compared to the PCs and SM possibly because LPCs can be less solvated with MeOH. However, for LPCs' $[M+Na]^+$ ions a higher MeOH ratio in the mobile phase improved the signal intensity. As Fig. 4B shows, the signal intensity of the $[M+Na]^+$ ion was significantly elevated when the ACN/MeOH ratio changed from 100/0 to 70/30–60/40, followed by a trend that moderately increased with a further increase in the MeOH ratio. The MeOH mobile phase system favored the formation of the sodium adduct when compared to the ACN system in the determination of steroids [32,33]. Perhaps this was due to ACNs lower dielectric constant and/or more complete solvation with the sodium ion via the cyanide functional group, which can reduce the availability of sodium ions for adduct formation. The mobile phase composition shifted towards a predominated amount of MeOH; therefore, it was beneficial for the

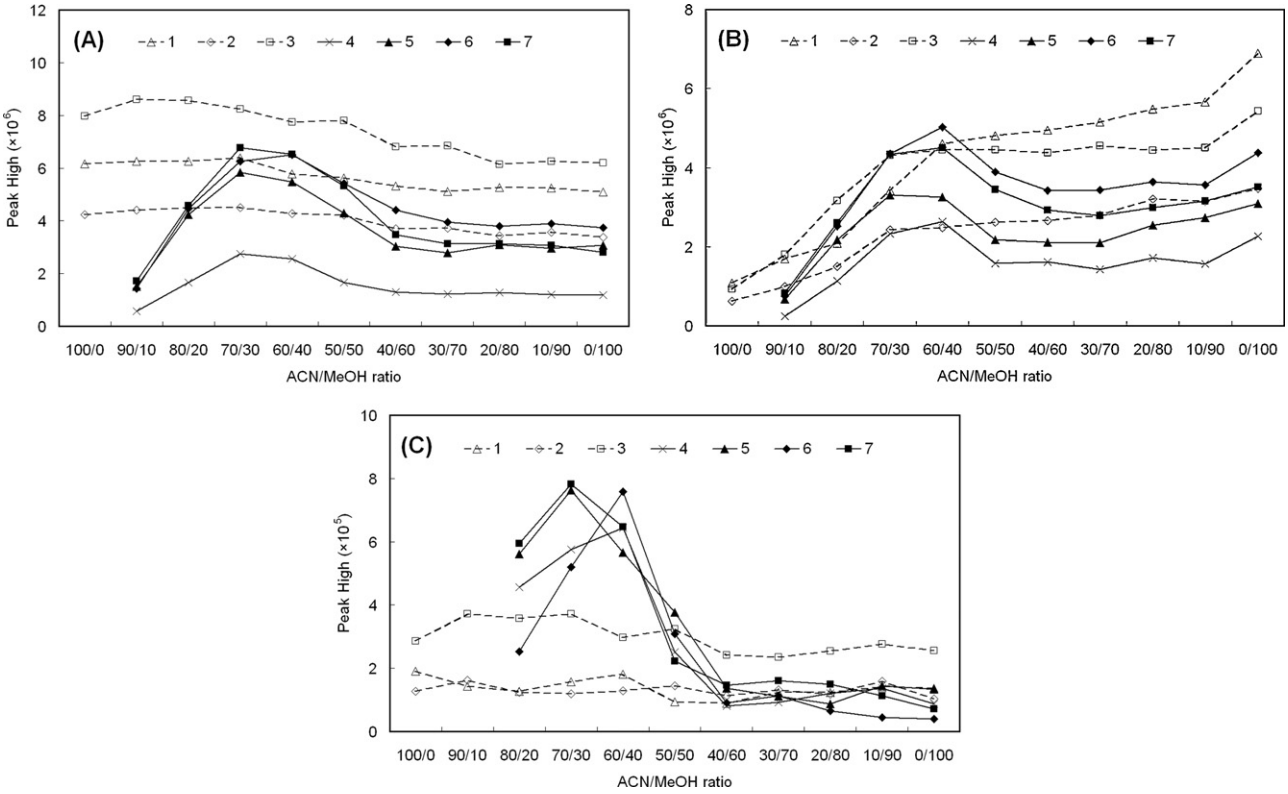

Fig. 4. The effect of the ACN/MeOH composition on the mobile phase for the signal intensity of (A) $[M+H]^+$, (B) $[M+Na]^+$ and (C) $[M-Me]^-$. The analyzed phosphocholines included the following: 1, PC(16:0/0:0); 2, PC(O-16:0/0:0); 3, PC(P-18:0/0:0); 4, SM(*d*18:1/17:0); 5, PC(16:0/16:0); 6, PC(O-16:0/16:0); 7, PC (P-18:0/18:1).

formation of $[M+Na]^+$ ion. This situation was also observed for the PCs and SM of $[M+Na]^+$ ions; the signal intensity slightly increased when the MeOH ratio increased beyond 70% in the mobile phase.

Fig. 5 shows the effect of the NH_4Ac content in the mobile phase to the phosphocholines signal response. Desirable signal intensities were reached for the LPCs when the concentration of the NH_4Ac in the mobile phase for each molecular ion ranged from 0.05 to 0.2 mM. Afterwards, a clear decline in the signal intensity was observed as the NH_4Ac concentration of the mobile phase increased above 0.2 mM (except for the PC(O-16:0/0:0) sodium adduct ion that was above 1 mM). Up to a certain extent, a concentration increase of the salt additive in the mobile phase can improve the signal intensity due to the elevation in excess charge on the spray droplet. This was caused by the elevation in the spray current, which was a function of the conductivity in the mobile phase [34]. Furthermore, the adequate conductivity in the solution reduced the size of the produced droplet in the spray process and increased the fraction of the excess charge ions at the droplet surface, which was favorable in the production of gaseous ions [31,35]. The concentration of the salt additive in the mobile phase was beyond some threshold, and this would cause a decline of the efficiency in converting excess charge to gaseous ions. The excess salt additive resulted in a visible increase in the size of the charged droplet. The droplet possessed a larger diameter and a smaller solvent evaporation rate was observed because the colligative solution properties reduced the efficiency in the desolvation process and the formation of the offspring droplets and finally, gaseous ions [30,31]. As the LPC result showed, this threshold where the signal suppression appeared at approximately 0.2 mM of NH_4Ac coincided with the chromatographic improvement of the PCs and SM (Fig. 2). Thus, the ionization suppression was offset to the chromatographic elevation in the signal sensitivity of the PCs and SM. Therefore, as shown in Fig. 5C, the $[M-Me]^-$ ion intensity of the PCs and SM only had a moderate elevation at NH_4Ac content ranging from 0.2 to 10 mM in the mobile phase. However, a very small signal change was observed for the $[M+H]^+$ ions of PCs and SM with an increase of the NH_4Ac content in the mobile phase (Fig. 5A), in which the chromatographic improvement in the signal sensitivity was almost neutralized. Clearly, some factors in the ionization process existed to further repress the $[M+H]^+$ ion intensity. It is possible that the competition occurred between both H^+ and Na^+ adduct formation in the process of electrospray ionization in which the formation of the Na^+ adduct became more favorable within such NH_4Ac content in the mobile phase. Hence, as Fig. 5B shows, the $[M+Na]^+$ ion intensity of PCs and SM are further elevated and the higher signal intensity could be found when the mobile phase existed at 1–2 mM of NH_4Ac (1–5 mM for SM). Simultaneously, a drop appeared in the $[M+H]^+$ ion intensity at thus NH_4Ac content. The mobile phase containing 10 mM of NH_4Ac was suggested for quantitative measurement through precursor ion scan of the product ion (at *m*/*z* 184) produced from the $[M+H]^+$ ion, while 1–2 mM NH_4Ac in the mobile phase could be use for the acquisition of the product ion spectra that was derived from the fragmentation of the $[M+Na]^+$ or the $[M-Me]^-$ ion for the molecular structure determination. The consideration of the shift in peak retention time due to the adaptation of the NH_4Ac content can be ignored because the shift of retention time was within variations of replicated measurements.

3.3. GPCs molecular structure determination

The phosphocholines had a common feature on the nature of the head group, which was the formation of a obvious signal at *m*/*z* 184, corresponding to the phosphorylcholine ion in their product ion spectra of $[M+H]^+$ [36]. Based on this fragment ion, the precursor ion scan of *m*/*z* 184 was chosen for preliminary phosphocholines profiling under positive ion mode. Based on preliminary phosphocholines profiling, constructed by the pair of *m*/*z* values and retention times, the product ion spectra was acquired for the

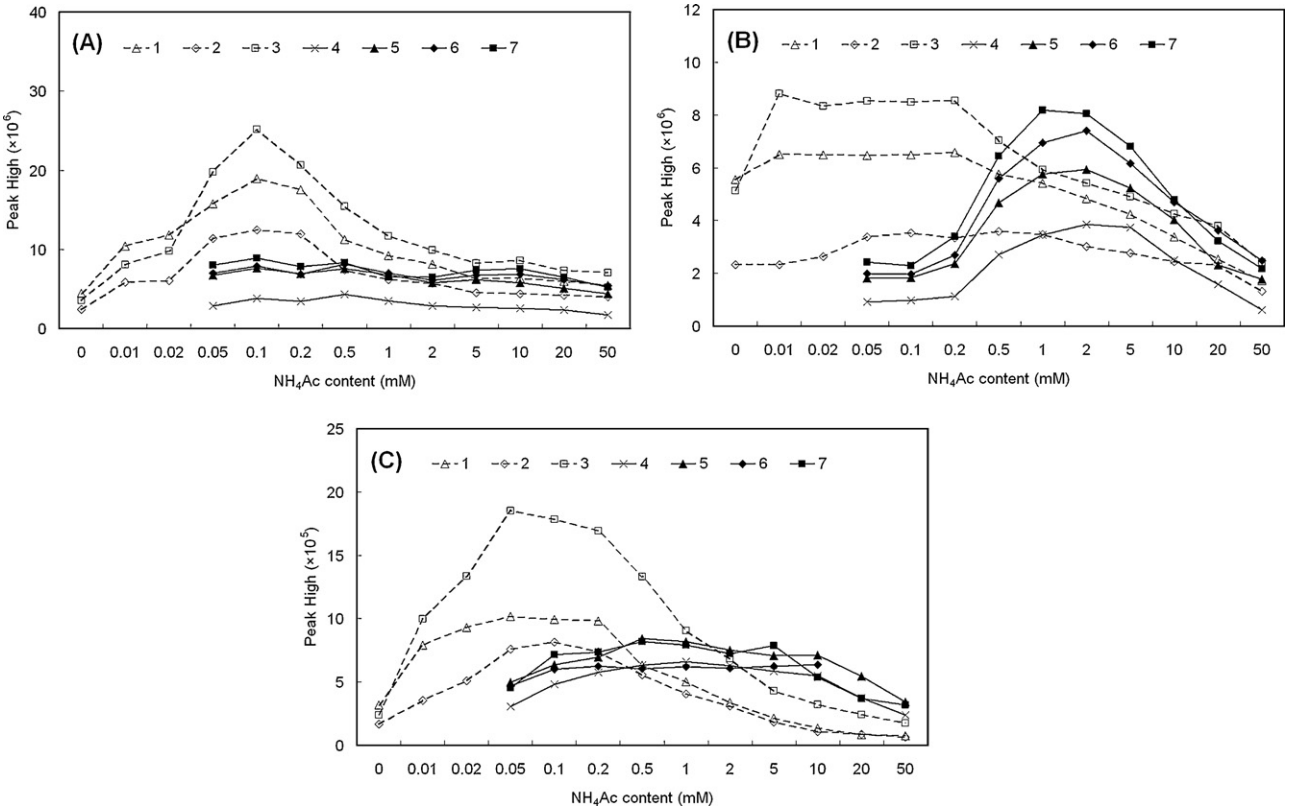

Fig. 5. The effect of the NH_4Ac content on the mobile phase for the signal intensity of (A) $[M+H]^+$, (B) $[M+Na]^+$ and (C) $[M-Me]^-$. The analyzed phosphocholines included the following: 1, PC(16:0/0:0); 2, PC(O-16:0/0:0); 3, PC(P-18:0/0:0); 4, SM(*d*18:1/17:0); 5, PC(16:0/16:0); 6, PC(O-16:0/16:0); 7, PC (P-18:0/18:1).

description of the molecular structure in which the signal with odd *m*/*z* were picked; SM was chosen based on the nitrogen rule. The PCs and LPCs were initially distinguished via the distinct region of retention time in the chromatogram. For a detail illustration of the molecular structure, the product ion spectra of $[M+H]^+$ was acquired and employed to determine the LPC subclass. As shown in Fig. 6, those spectra derived from different LPC subclasses were distinction and contained unique product ions and relative intensities of ion signal. For example, the base ion at *m*/*z* 184 was used to distinguish the acyl-LPC, for both the base ion of alkyl- and alk-1-enyl-LPC were at *m*/*z* 104 (corresponding to choline) [37] that the ion intensity was approximately 5 times higher than that at *m*/*z* 184. The acyl-LPC regioisomers were appreciated by the comparison of both product ions at *m*/*z* 184 and 104 in which both ions were predominant in the spectrum for the *sn*-2-LPC (Fig. 6A). The *sn*-1-LPC had just one predominant product ion at *m*/*z* 184 with minor ion intensity at *m*/*z* 104 (Fig. 6B). The acyl-LPC regioisomers were also distinctly separated by chromatography by first eluding the *sn*-1-LPC. The alkyl- and alk-1-enyl-LPC can be discriminated based on whether the spectrum presented the ions at *m*/*z* 240 (corresponding to the neutral loss of aldehyde from the *sn*-1 position) and 181 (corresponding to the further neutral loss of trimethylamine from the ion at *m*/*z* 240) [38] or not; as shown in Fig. 6C, the spectrum acquired from alkyl-LPC did not show those two ion signals. Once the subclass was assigned, the carbon number and the degree of unsaturation possessed in the fatty acid substituent of LPC can be informed through the deductive inference of the molecular weight (structure). In addition, the content of the alkyl- and alk-1-enyl-LPC was relatively low in most biological tissues and the precursor ion scan of *m*/*z* 104 was combined for preliminary LPCs profiling. The product ion at *m*/*z* 104 was superiorly produced in the collision-induced fragmentation of the two LPC subclasses that had a contrast that was more than 5 times stronger compared to the product ion at *m*/*z* 184. In this case, however, both $[M+H]^+$ and $[M+Na]^+$ ions of the LPCs would be simultaneously recorded in the profile because the $[M+Na]^+$ ion can also produced the same product ion at *m*/*z* 104 in the fragmentation process, which should be obtained from the profile.

The product ion spectra of $[M+Na]^+$ was chosen to decide on the subclass of PCs in the present study. Fig. 7 shows that each PC subclass had similar components for product ions in the spectrum acquired from the fragmentation process of the $[M+Na]^+$ ion, which included the ions at *m*/*z* 86 and 147, respectively corresponding to a vinyltrimethylamine and a sodiated five-member cyclophosphane, the ions corresponding to the neutral loss of 59 ($[M+Na\text{-}N(CH_3)_3]^+$), 183 ($[M+Na\text{-}HPO_4(CH_2)_2N(CH_3)_3]^+$) and 205 ($[M+Na\text{-}NaPO_4(CH_2)_2N(CH_3)_3]^+$) from the $[M+Na]^+$ ion [37,39]. The relative intensity of the $[M+Na\text{-}183]^+$ and the $[M+Na\text{-}205]^+$ ions were clearly different among these PC subclasses, which can be a reliable start to subclass divisions. The predominant $[M+Na\text{-}183]^+$ ion (~90%) always accompanied the minor $[M+Na\text{-}205]^+$ ion (<40%) in the product ion spectrum of diacyl-PC, as was the case for PC(16:0/18:1), Fig. 7A. In contrast to diacyl-PC, the product ion spectra derived from the alkylacyl-PC and alk-1-enylacyl-PC sodium adducts revealed that the relative intensity at both the $[M+Na\text{-}183]^+$ and $[M+Na\text{-}205]^+$ ions are minor. Nevertheless, the ion intensity of $[M+Na\text{-}183]^+$ was always higher compared to the $[M+Na\text{-}205]^+$ ion in the product ion spectra produced from alk-1-enylacyl-PC (PC(P-18:0/18:1), Fig. 7C). The alkylacyl-PC showed that the $[M+Na\text{-}183]^+$ ion intensity was clearly lower than the $[M+Na\text{-}205]^+$ ion intensity, as was the case for PC(O-16:0/16:0), Fig. 7B; both ions intensity were always less than 50% of the base ion.

Once the PC subclass was decided, the description in its fatty acid substituent was accomplished via further illustrating the product ion spectrum of $[M-Me]^-$ and by deductively inferring the molecu-

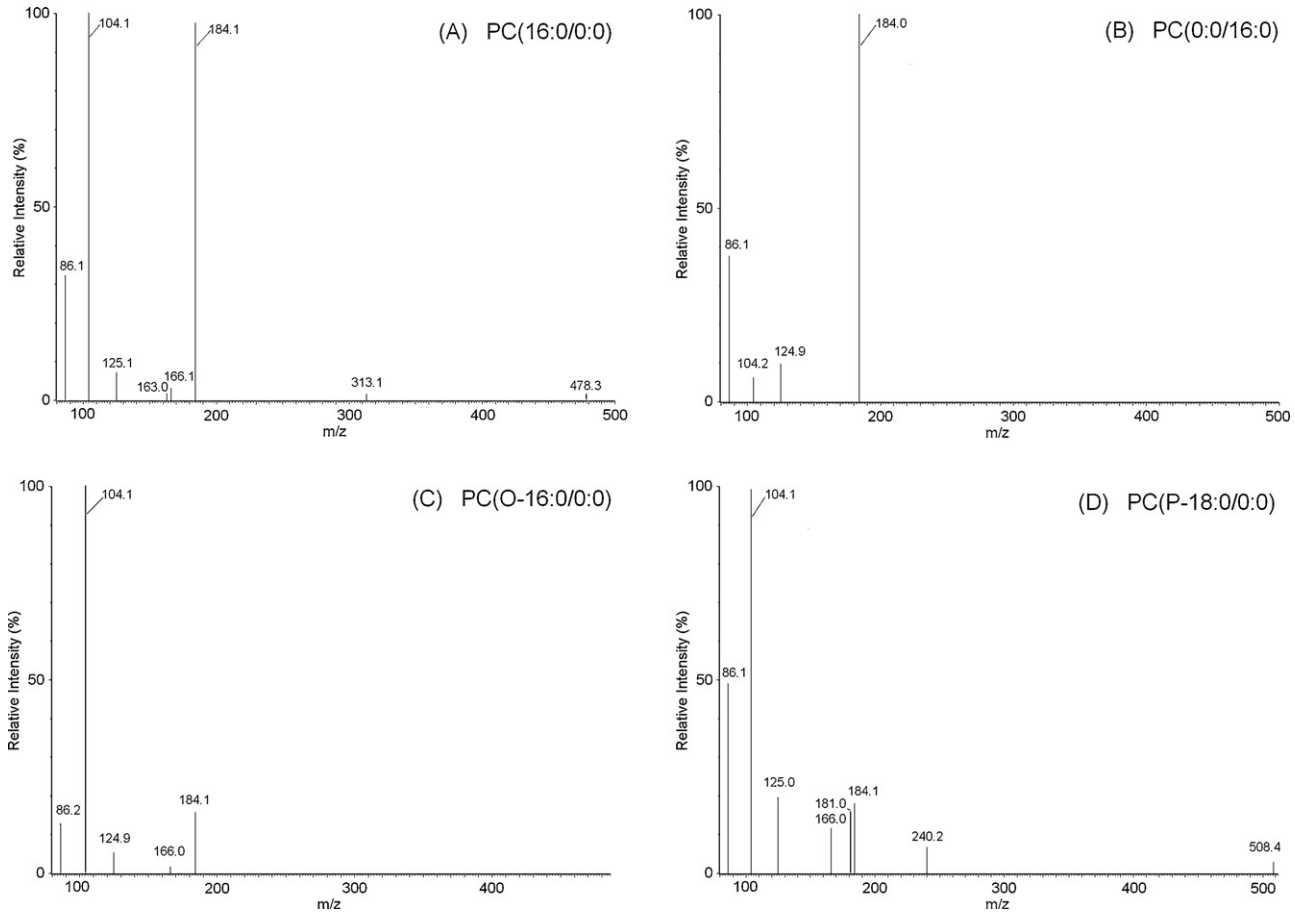

Fig. 6. Collision-induced fragmentation spectra of the $[M+H]^+$. The selected LPC molecular ions were collided with argon (0.1 mL/min) using a collision energy of 30 eV by the rf-only quadrupole.

lar weight (structure). Under negative ion mode, the molecular ion $[M-Me]^-$ was produced via the loss of one methyl moiety from the choline head group of PCs, which can generated the useful product ions in the fragmentation process for determining fatty acid substituent existed in the PCs molecular structure. For example, the main product ions at *m*/*z* 281 and 255, corresponding to the 18:1- and 16:0-carboxylate anions for PC(16:0/18:1) were obtained as the deductive inference for describing the fatty acid substituent of the carbon number and the degree of unsaturation, Fig. 8A. The intensity of the *sn*-2 carboxylate anion (*m*/*z* 281) was approximately threefold higher than the intensity of the *sn*-1 carboxylate anion (*m*/*z* 255), which was the reason the *sn*-2 acyl group was easily loss [39]. Based on these characteristics, the linkage position of the acyl group in the diacyl-PC molecular structure was determined. The polyunsaturated carboxylate anion produced in the fragmentation process has been found to further undergo a strong secondary dissociation, while it does not occur easily for the saturated or less unsaturated carboxylate anions [40]. Such fragmentation characteristics cause a dramatic change in the signal intensity of polyunsaturated carboxylate anions. Fig. 8D shows a case derived from PC(16:0/22:6); the spectrum clearly contained the *sn*-1 and the *sn*-2 carboxylate anion signals at *m*/*z* 255 and 327 as well as the strong ion signal at *m*/*z* 283 that was produced via the further loss of CO_2 from the 22:6-carboxylate anion in the consecutive dissociation process. Clearly, this secondary dissociation process caused a drastic decline in the intensity of the *sn*-2 carboxylate anion at *m*/*z* 327 that was clearly lower than the intensity of the *sn*-1 carboxylate anion at *m*/*z* 255; this must be kept in mind when deciding on the position of the acyl substituent on the glycerol backbone.

A single carboxylate anion signal was presented in the spectra that were derived from the symmetrical diacyl-PC, alkylacyl-PC (Fig. 8B) or alk-1-enylacyl-PC (Fig. 8C), which reflect the essentiality of prior PCs subclass decision. The symmetrical diacyl-PC produced the same carboxylate anion from both the *sn*-1 and *sn*-2 positions and the cleavage of the ether or vinyl ether linkage in the alkylacyl-PC and alk-1-enylacyl-PC molecular did not occur easily [39]. It was still possible to achieve the description of the fatty acid substituent by performing mathematical calculations of the mass balance for the molecular weight (structure). Another route for the validation needed to be performed via the analysis of another product ion that corresponded to the neutral loss of the fatty acyl substituent at the *sn*-2 position as an acid ($[M-Me\text{-}R_2CH_2COOH]^-$) and ketene ($[M-Me\text{-}R_2CHCO]^-$) from the $[M-Me]^-$ ion [39], such as the ions at *m*/*z* 448 and 466 shown in Fig. 8B, to ensure the accuracy of determined molecular structure of alkylacyl-PC and alk-1-enylacyl-PC.

3.4. Performance of the analytical method

The performance of analytic method was presented via several items of quality assessment using the probing GPCs. Calibration curves were created through directly measuring a series of GPCs standard solution in different concentrations. As shown in Table 1, a good correlation of linearity in the measured signal response corresponding to the lipid quantity was exhibited. The performing linear range was 0 (blank)–10 ng/μL with correlation coefficients ranging from 0.9983 to 0.9997 (for a 10-point calibration curve). The sensitivities (slope of the calibration curve) achieved for each GPC were within the range of 57,009–375,454 μL/ng. Limits of detection (LOD) were based on three times the standard deviation of seven

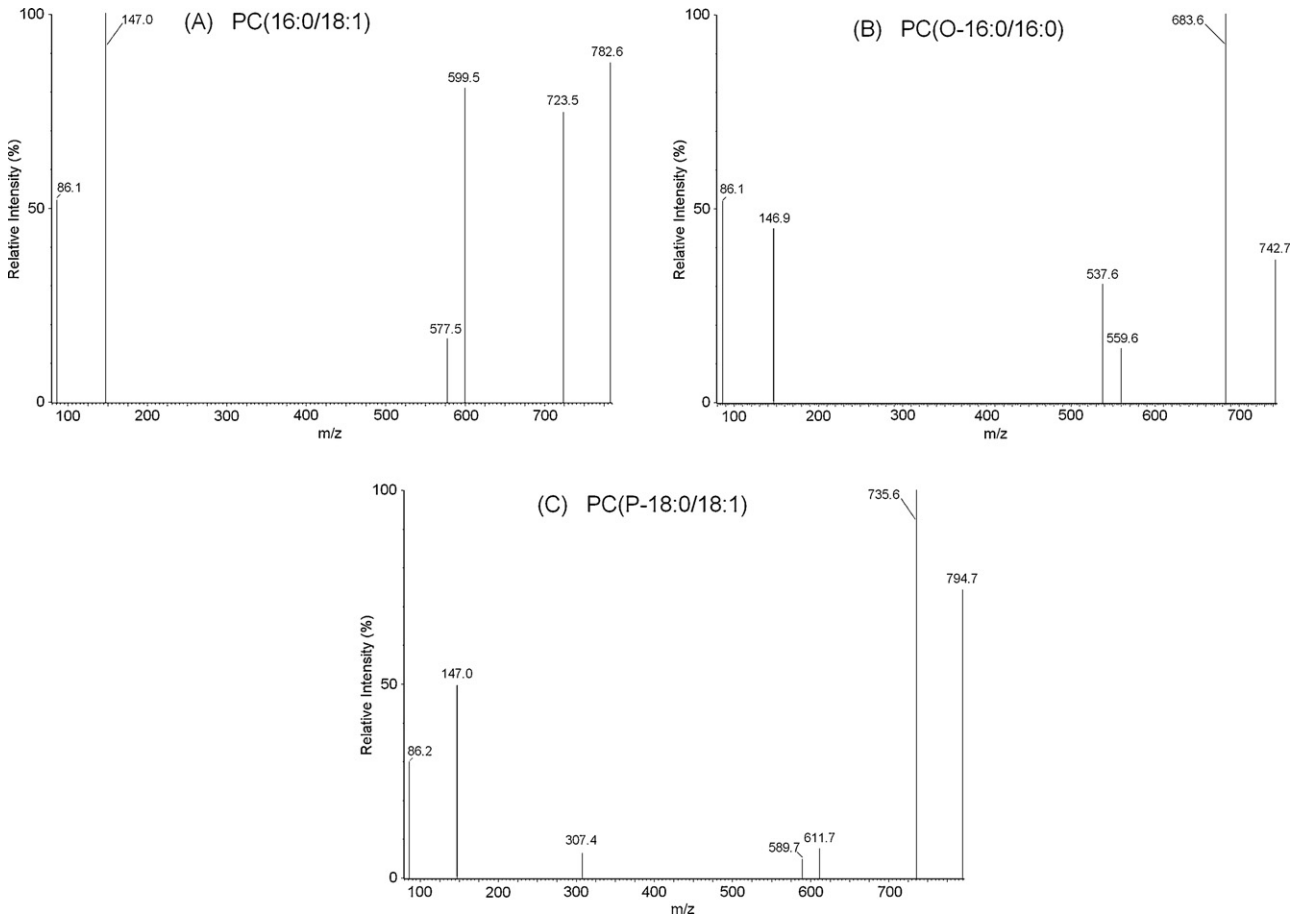

Fig. 7. Collision-induced fragmentation spectra of the $[M+Na]^+$. The selected PC molecular ions were collided with argon (0.1 mL/min) using a collision energy of 28 eV by the rf-only quadrupole.

replicate determinations of the standard solution that was used for the LPCs (0.02 ng/μL), and for PCs (0.005 ng/μL). The LOD ranged from 0.002 to 0.016 ng/μL in which the LOD of the PCs was approximately a half order better compared to the LPCs. The recovery of the GPCs from the 1.0 mg lung tissue samples was calculated by comparing to the spiked lipid quantity of 0.2 μg. The mean recovery rates and the standard deviations obtained from the three replicate analyses are shown in Table 1 in which the acceptable recoveries were obtained in the range of 84–116% with variations of less than 10%.

Table 1
The performance of the analytical method using optimized conditions.

Lipid	Calibration equation	Correlation coefficient	Recovery rate (%)	LOD (ng/μL)
PC(16:0/0:0)	$y = 57{,}009x$	0.9983	84 ± 9	0.016
PC(O-16:0/0:0)	$y = 78{,}380x$	0.9997	90 ± 9	0.011
PC(P-18:0/0:0)	$y = 72{,}793x$	0.9986	101 ± 8	0.012
PC(18:0/18:0)	$y = 297{,}102x$	0.9991	84 ± 8	0.003
PC(O-16:0/16:0)	$y = 375{,}454x$	0.9984	88 ± 4	0.002
PC(P-18:0/18:1)	$y = 336{,}639x$	0.9992	116 ± 5	0.002

The 10-point calibration curves were made with a double concentration elevating interval from 0 (blank) to 10 ng/μL. Recovery rate were presented as the mean ± standard deviation ($n = 3$), which the recoveries of lipids from 1.0 mg lung tissue were calculated by comparing the spiked lipid quantity (0.2 μg). Limits of detection (LOD) were based on three times the standard deviation of seven replicate experiments using the standard solutions at 0.02 ng/μL for LPCs and at 0.005 ng/μL for PCs.

3.5. Application of the method used to analyze GPCs in preterm mice

The verification in the practical usability of the analytical method has also been conducted via the study of VEGF-induced early lung maturation in the premature mouse model. The increase of the GPCs as a surfactant lipid in lungs has been found to be one of the indicators of lung maturation [41]. Measurements of GPCs can provide the final metabolic status in the lung developmental process to cross confirm with other physiological indicators. The comprehensive profiling of GPCs can provide an insight into the understanding of the chemically induced early lung maturation. The analysis of variation for the profiling of the GPCs was ana-

Table 2
The examples of major (>1%) and minor (<0.1%) glyserophosphocholine molecular species existed in the fetal mouse lungs.

Major species	Percentage (%)[a]	Minor species	Percentage (%)
PC(16:0/16:0)	14.37	PC(14:0/15:0)	0.10
PC(16:0/18:1)	12.26	PC(22:6/22:6)	0.08
PC(16:0/16:1)	8.90	PC(O-14:0/16:1)	0.07
PC(16:0/20:4)	5.07	PC(0:0/18:2)	0.06
PC(16:0/22:6)	3.59	PC(0:0/22:6)	0.03
PC(O-16:0/16:0)	1.72	PC(0:0/16:1)	0.02
PC(16:1/18:2)	1.51	PC(16:1/0:0)	0.02
PC(P-16:0/16:0)	1.12	PC(22:6/0:0)	0.01
PC(18:0/22:6)	1.03	PC(O-16:0/0:0)	0.01
PC(18:2/18:2)	1.00	PC(P-18:0/0:0)	0.01

[a] Percentage is the mean ratio ($n = 8$) of signal intensity of glyserophosphocholine molecular species for the total identified species in the E18.5 fetal mouse lungs.

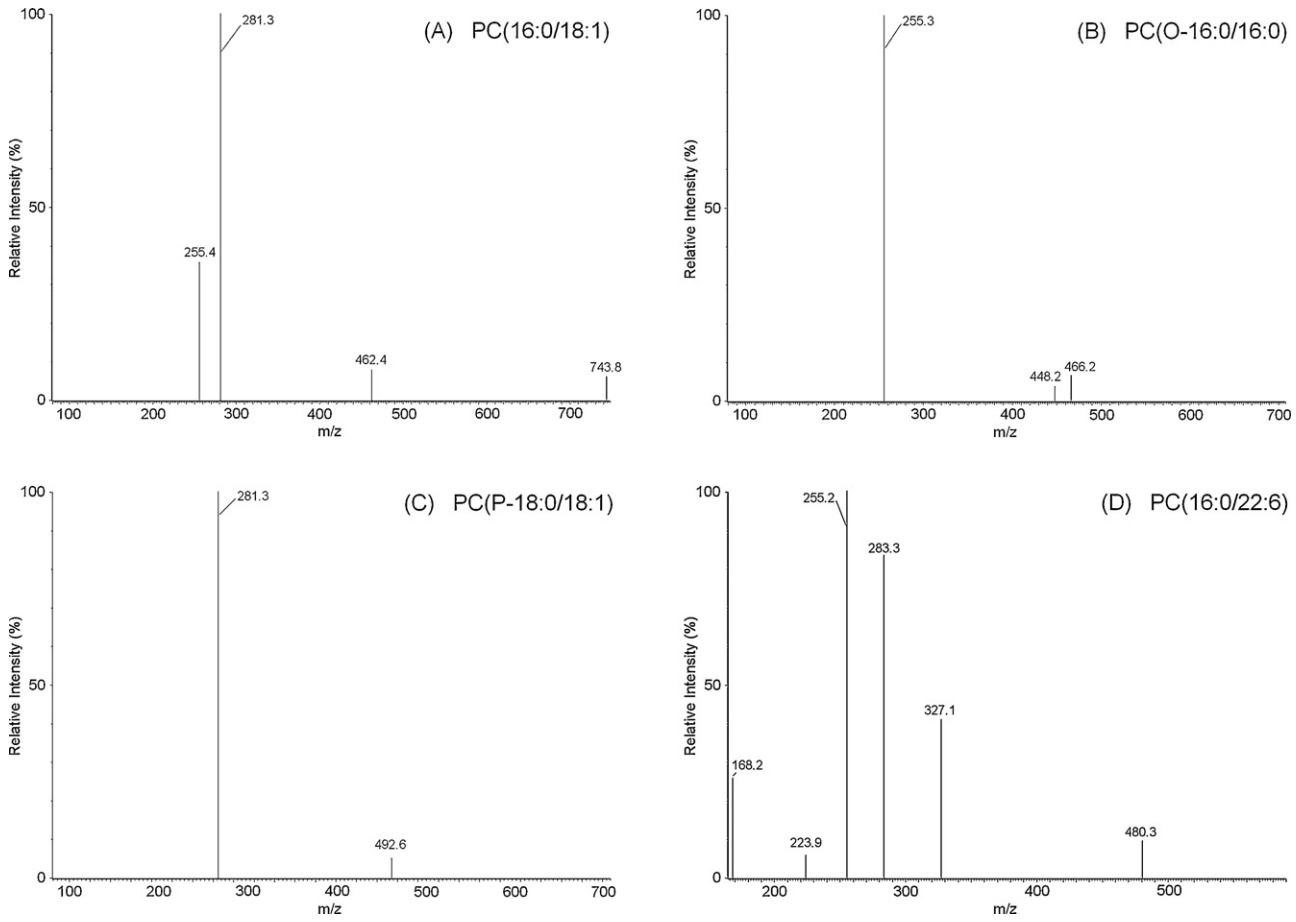

Fig. 8. Collision-induced fragmentation spectra of the $[M-Me]^-$. The selected PC molecular ions were collided with argon (0.1 mL/min) using a collision energy of 30 eV by the rf-only quadrupole.

lyzed prior to the experiment by three replicate measurements of eight E18.5 fetal mouse lungs delivered from the same pregnant mouse. As Fig. 9 shows, the variation of GPCs profile in the chemical measurement and the individual biological replications were acceptable, which was based on the congregate degree of data points in the PCA score plot. The total 93 GPCs molecular species were identified in the profile in which the content of GPCs showed a great difference among each molecular species. Ten chose major (>1%) and minor (<0.1%) GPCs molecular species are listed in Table 2. The relative amount of GPCs was more than three orders from 14.37% to less than 0.01% that is calculated via the normalization of the total GPCs signal. These results revealed that the proposed analytical method possessed desirable determining capabilities for the profiling of GPCs. This analytical procedure was then repeated to obtain the GPCs profiling of the lung tissue in the treatment and control groups.

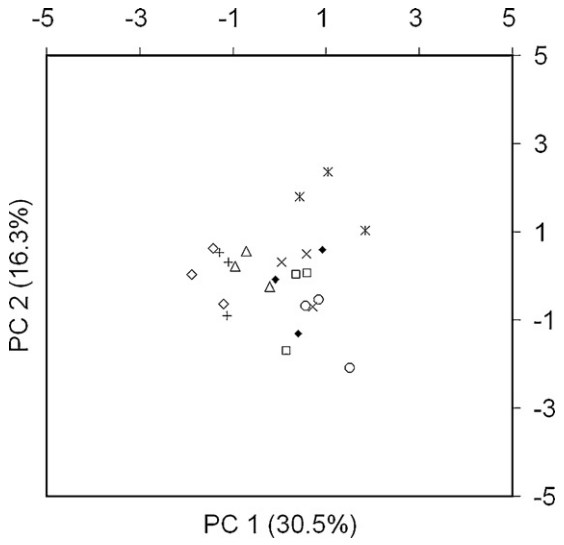

Fig. 9. The score plot of principal component analysis, which showed the variation of glyserophosphocholines profiling in the three replicate measurements of eight E18.5 fetal mouse lungs derived from the same pregnant mouse.

As shown in Fig. 10, the score plot of PCA was performed using the mean value of three replicate measurements of GPCs profile of the lung tissue; lung samples were respectively derived from the control and VEGF agonist-treated E18.5 fetal mice. The result showed that clear differences in the GPCs molecular composition of lung tissue existed between these two groups. Compare to the control group, as shown in Table 3, the VEGF agonist-treated preterm fetal pups presented a significant increase in the content of PCs with saturated or less unsaturated fatty acid substituent in the lung tissue; the amount of the acyl-LPC and diacyl-PC with the polyunsaturated fatty acid substituent located at the *sn*-2 position showed a significant decrease. PCs are membrane phospholipid metabolites that have been regarded as an important factor for organ development, in which the unsaturated degree of fatty acid substituent influences many crucial cellular functions [42]. Lysophospholipids, such as LPCs, have been recognized as participants in the phospholipids metabolic process and the important intercellular signaling molecules in which they regulate precise cellular functions and

Table 3
The change of glyserophosphocholine content in the VEGF agonist-treated fetal mice lungs vs. to the control group.[a]

Identified species	%Change	Identified species	%Change	Identified species	%Change
PC(14:0/14:0)	↑68	PC(18:6/16:0)	↑22	PC(16:0/19:5)	↓32
PC(14:0/15:0)	↑53	PC(20:1/18:1)	↑11[b]	PC(16:0/20:4)	↓12
PC(15:0/16:0)	↑26[b]	PC(16:0/22:2)		PC(18:0/20:4)	↓21
PC(16:0/15:0)		PC(18:0/20:2)		PC(18:1/20:4)	↓17
PC(15:0/16:1)	↑36	PC(22:2/16:0)		PC(18:1/22:6)	↓10
PC(15:0/18:2)	↑21[b]	PC(22:0/18:1)	↑18	PC(18:2/18:2)	↓7
PC(16:1/17:1)		PC(34:6)	↑112	PC(18:2/20:4)	↓30
PC(17:1/16:1)		PC(28:1)	↑104	PC(15:0/0:0)	↓42
PC(16:0/14:0)	↑29	PC(30:3)	↑64	PC(16:0/0:0)	↓30
PC(16:0/16:1)	↑16	PC(O-14:0/16:0)	↑38[b]	PC(0:0/16:0)	↓29
PC(16:0/18:2)	↑7[b]	PC(O-16:0/14:0)		PC(18:0/0:0)	↓34
PC(16:1/18:1)		PC(O-14:0/16:1)	↑37	PC(0:0/18:0)	↓41
PC(16:0/22:6)	↑8	PC(O-14:1/16:0)	↑20	PC(18:1/0:0)	↓36
PC(16:1/14:0)	↑47	PC(O-15:1/18:3)	↑37	PC(0:0/18:1)	↓17
PC(16:1/16:1)	↑31	PC(O-16:0/16:0)	↑11	PC(18:2/0:0)	↓56
PC(16:1/18:2)	↑14	PC(O-18:0/16:0)	↑20	PC(0:0/18:2)	↓30
PC(16:1/22:6)	↑14	PC(O-18:1/18:1)	↑24[b]	PC(20:0/0:0)	↓38
PC(17:0/18:1)	↑19	PC(O-18:0/18:2)		PC(20:4/0:0)	↓64
PC(17:0/18:2)	↑14	PC(O-18:2/16:0)	↑36[b]	PC(0:0/20:4)	↓41
PC(17:1/16:0)	↑20[b]	PC(O-18:1/16:1)		PC(22:6/0:0)	↓34
PC(15:0/18:1)		PC(P-16:0/16:1)	↑17		
PC(18:0/18:0)	↑6	PC(P-16:0/18:1)	↑17		
PC(18:0/18:1)	↑12[b]	PC(P-20:0/16:0)	↑38		
PC(20:1/16:0)					

[a] A one-way analysis of variance was used to assess the significant difference ($p < 0.05$) of the glyserophosphocholine content in E18.5 fetal mice lungs between the VEGF agonist-treated and the control group.
[b] The content change was contained as the isobaric glyserophosphocholine molecular species.

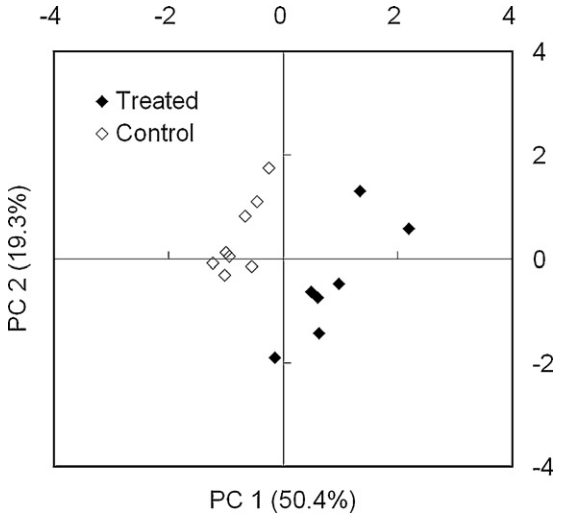

Fig. 10. The score plot of principal component analysis, which showed distinguishable profile of the glyserophosphocholines in the E18.5 fetal mouse lung between the control and VEGF agonist-treated groups. Three replicate measurements were conducted for all lung tissue samples.

have been reported to signal through membrane-bound receptors to activate many signaling pathways [43]. Lysophospholipids and their receptors are presented in a wide range of cell types and tissues that showing their importance in various physiological processes, such as reproduction and development. Changes in such GPCs levels suggested that the antenatal intra-amniotic VEGF agonist treatment caused a modification in the specific GPCs metabolic process in the fetal mouse lung. This data suggested that the intra-amniotic VEGF agonist treatment induced a metabolic change in GPCs in the fetal mouse lungs.

4. Conclusion

The comprehensive profiling of GPCs can reflect the changes in organ function, physiological requirements and can provide a greater understanding of the cell metabolic process. A two-phase analytical procedure has been established in the present study for the comprehensive profiling of GPCs in the biological tissue. After optimization of the parameters, the performance of this proposed analytical procedure was obviously elevated. The practical usability of the analytical procedure was also verified through the study of chemically induced early lung maturation in which significant GPCs that indicate lung maturation were characterized at the level of their molecular structures. Based on the results of performance and reliability analysis, this proposed analytical procedure was dependable for GPCs profiling of lung tissue. The analytical procedure may also be extended to other tissues for the profiling of GPCs after the verification of practical usability.

Acknowledgements

The research was supported by National Health Research Institutes (NHRI-EX99-9915EC) in Taiwan.

References

[1] G. van Meer, D.R. Voelker, G.W. Feigenson, Nat. Rev. Mol. Cell Biol. 9 (2008) 112.
[2] C.D. Stubbs, A.D. Smith, Biochim. Biophys. Acta 779 (1984) 89.
[3] J.R. Hazel, E.E. Williams, Prog. Lipid Res. 29 (1990) 167.
[4] L.J. Robers II, Cell. Mol. Life Sci. 59 (2002) 727.
[5] S. Brooks, G.T. Clark, S.M. Wright, R.J. Trueman, A.D. Postle, A.R. Cossins, N.M. Maclean, J. Exp. Biol. 205 (2002) 3989.
[6] S. Schuck, M. Honsho, K. Ekroos, A. Shevchenko, K. Simons, Proc. Natl. Acad. Sci. U.S.A. 100 (2003) 5795.
[7] B.P. Hurley, B.A. McCormick, Infect. Immun. 76 (2008) 2259.
[8] Y. Masuzawa, T. Sugiura, H. Sprecher, K. Waku, Biochim. Biophys. Acta 1005 (1989) 1.
[9] J.D. Winker, A.N. Fonteh, C.M. Sung, J.D. Heravi, A.B. Nixon, M. Chabot-Fletcher, D. Grisword, L.A. Marshall, F.H. Chilton, J. Pharmacol. Exp. Ther. 274 (1995) 1338.
[10] L.V. Chernomordik, S.S. Voegl, A. Sokoloff, H.O. Onaran, E.A. Leikina, J. Zimmerberg, FEBS Lett. 318 (1993) 71.
[11] P.B. Corr, J.E. Saffitz, B.E. Sobel, Basic Res. Cardiol. 82 (1987) 199.
[12] M. Sakai, A. Miyazaki, H. Hakamata, T. Kodama, H. Suzuki, S. Kobori, M. Shichiri, S. Horiuchi, J. Biol. Chem. 271 (1996) 27346.
[13] Y. Xu, Biochim. Biophys. Acta, Mol. Cell. Biol. 1582 (2002) 81.
[14] W. Anna, K. Ulrike, H. Michael, H. Joachim, W. Oksana, H. Marion, F. Klaus, S. Andrea, K. Jochen, Neurobiol. Aging 25 (2004) 1299.

[15] M. Milkevitch, H. Shim, U. Pilatus, S. Pickup, J.P. Wehrle, D. Samid, H. Poptani, J.D. Glickson, E.J. Delikatny, Biochim. Biophys. Acta 1734 (2005) 1.
[16] O. Zaccheo, D. Dinsdale, P.A. Meacock, P. Glynn, J. Biol. Chem. 279 (2004) 24024.
[17] T.R. Warne, M. Robinson, Lipids 25 (1990) 748.
[18] C.J. DeLong, P.R.S. Baker, M. Samuel, Z. Cui, M.J. Thomas, J. Lipid Res. 42 (2001) 1959.
[19] J. Bielawski, J.S. Pierce, J. Snider, B. Rembiesa, Z.M. Szulc, A. Bielawska, Adv. Exp. Med. Biol. 688 (2010) 46.
[20] J.M. Halket, D. Waterman, A.M. Przyborowska, R.K.P. Patel, P.D. Fraser, P.M. Bramley, J. Exp. Bot. 56 (2005) 219.
[21] M.C. Sullards, E. Wang, Q. Peng, A.H. Merrill Jr., Cell. Mol. Biol. 49 (2003) 789.
[22] S.L. Abidi, T.L. Mounts, J. Chromatogr. 598 (1992) 209.
[23] I.D. Wilson, J.K. Nicholson, J. Castro-Perez, J.H. Granger, K.A. Johnson, B.W. Smith, R.S. Plumb, J. Proteome Res. 4 (2005) 591.
[24] K. Retra, O.B. Bleijerveld, R.A. van Gestel1z, A.G.M. Tielens, J.J. van Hellemond, J.F. Brouwers, Rapid Commun. Mass Spectrom. 22 (2008) 1853.
[25] V. Compernolle, K. Brusselmans, T. Acker, P. Hoet, M. Tjwa, H. Beck, S. Plaisance, Y. Dor, E. Keshet, F. Lupu, B. Nemery, M. Dewerchin, P.V. Veldhoven, K. Plate, L. Moons, D. Collen, P. Carmeliet, Nat. Med. 8 (2002) 702.
[26] J. Folch, M. Lees, G.H.S. Stanley, J. Biol. Chem. 226 (1957) 497.
[27] C.Y. Lin, H. Wu, R.S. Tjeerdema, M.R. Viant, Metabolomics 3 (2007) 55.
[28] D.V. McCalley, J. Chromatogr. A 708 (1995) 185.
[29] J.H. Park, A.J. Dallas, P. Chau, P.W. Carr, J. Phys. Org. Chem. 7 (1994) 757.
[30] P. Kebarle, L. Tang, Anal. Chem. 65 (1993) 972A.
[31] T.L. Constantopoulos, G.S. Jackson, C.G. Enke, J. Am. Soc. Mass Spectrom. 10 (1999) 625.
[32] Y.C. Ma, H.Y. Kim, J. Am. Soc. Mass Spectrom. 8 (1997) 1010.
[33] A. Marwah, P. Marwah, H. Lardy, J. Chromatogr. A 964 (2002) 137.
[34] L. Tang, P. Kebarle, Anal. Chem. 63 (1991) 2709.
[35] J.F. Fernandez De La Mora, I.G.J. Loscertales, J. Fluid Mech. 260 (1994) 155.
[36] X. Han, R.W. Gross, Mass Spectrom. Rev. 24 (2005) 367.
[37] F.F. Hsu, J. Turk, A.K. Thukkani, M.C. Messner, K.R. Wildsmith, D.A. Ford, J. Mass Spectrom. 38 (2003) 752.
[38] N. Khaselev, R.C. Murphy, J. Am. Soc. Mass Spectrom. 11 (2000) 283.
[39] X. Han, R.W. Gross, J. Am. Soc. Mass Spectrom. 6 (1995) 1202.
[40] F.F. Hsu, J. Turk, J. Am. Soc. Mass Spectrom. 11 (2000) 986.
[41] W.M. Maniscalco, C.M. Wilson, I. Gross, L. Gobran, S.A. Rooney, J.B. Warshaw, Biochim. Biophys. Acta Lipids Lipid Metab. 530 (1978) 333.
[42] H. Ariyama, N. Kono, S. Matsuda, T. Inoue, H. Arai, J. Biol. Chem. 285 (2010) 22027.
[43] E. Birgbauer, J. Chun, Cell. Mol. Life Sci. 63 (2006) 2695.